Real-Time Imaging of Cell-Surface Proteins with Antibody-Based Fluorogenic Probes

Wenchao Wang,[+a] Ying Zhang,[+a] Hong Zhao,[+a] Xinlei Zhuang,[a] Haoting Wang,[a] Kaifeng He,[ab] Wanting Xu,[a] Yu Kang,[a] Shuqing Chen,[a] Su Zeng[ab] and Linghui Qian*[ab]

Supporting Information

Table of contents **Page**

I. General information

All reagents were purchased from commercial suppliers and used without further purification unless otherwise noted. All reactions were carried out under an ambient atmosphere; exclusion of air or moisture was not required. For thin layer chromatography (**TLC**), Qingdao Bangkai Hi-tech Materials Co., Ltd TLC plates (HSGF 254) were used, and compounds were visualized with a UV light. Flash column chromatography was carried out using silica gel 60F (Qingdao Haiyang Chemical co., Ltd). **^{1}H** and **^{13}C NMR** spectra were recorded on a Bruker AVIII 500M (500 MHz) spectrometer. Chemical shifts were reported in parts per million (ppm), and the residual solvent peak was used as an internal reference: ^{1}H (chloroform δ 7.26; DMSO δ 2.50), ^{13}C (chloroform δ 77.16; DMSO δ 39.52). Data are reported as follows: chemical shift, multiplicity (s = singlet, d = doublet, t = triplet, q = quartet, m = multiplet, br = broad, dd = doublet of doublets), coupling constants (Hz) and integration. High-resolution mass spectra were measured on an Agilent 6200 Series TOF and 6500 Series LC-MS. Cetuximab (Erbitux®, 5mg/mL) was purchased from Merck. Necitumumab was expressed and purified by Xinlei Zhuang (Prof. Shuqing Chen's lab, College of Pharmaceutical Sciences, Zhejiang University). Human immunoglobulin G (IgG) was purchased from Shanghai Acmec Biochemical Co., Ltd. Recombinant EGFR (extracellular domain; ATMP00496HU) was purchased from Atagenix.

II. Chemical synthesis

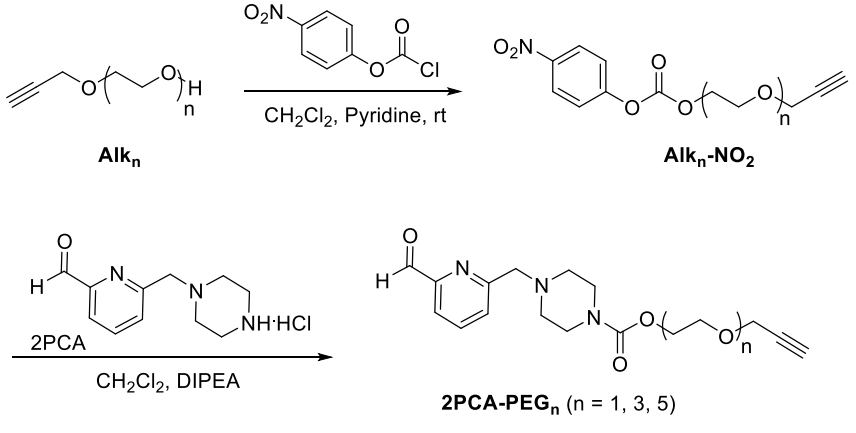

Scheme S1. Synthesis of **2PCA-PEG$_n$**.

General procedure.

(1) To a solution of **Alk$_n$** (0.5 mmol) in dry CH_2Cl_2 (4 mL) was added 4-nitrophenyl chloroformate (400mg, 2 mmol) followed by pyridine (160 μL, 2 mmol) via syringe at 0 ^oC. The reaction was stirred overnight at room temperature and transferred to a separatory funnel with additional CH_2Cl_2 (40 mL) and saturated copper sulfate solution (3 × 100 mL). The organic layer was dried over Na_2SO_4 and the solvent was removed in vacuo. The residue was purified by flash chromatography (Alk_1-NO_2: CH_2Cl_2/PE = 1/3; Alk_3-NO_2: CH_2Cl_2/PE = 1/2; Alk_5-NO_2: CH_2Cl_2/PE = 1/1; PE is petroleum ether) to give the white solid **Alk$_n$-NO$_2$** (yields: **Alk$_1$-NO$_2$** 85%, **Alk$_3$-NO$_2$** 84%, **Alk$_5$-NO$_2$** 80%).

(2) **2PCA** (20 mg, 0.1 mmol)[S1] and DIPEA (0.6 mmol) were added into dry CH_2Cl_2 (2 mL), followed by addition of **Alk$_n$-NO$_2$** (0.13 mmol) at room temperature. The solution was stirred for overnight and purified by flash chromatography (CH_2Cl_2/CH_3CN = 10/1) to give the desired product **2PCA-PEG$_n$** (yields: **2PCA-PEG$_1$** 35%, **2PCA-PEG$_3$** 38%, **2PCA-PEG$_5$** 35%).

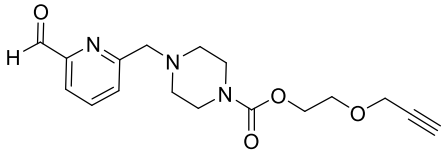

2PCA-PEG$_1$

^{1}H NMR (500 MHz, Chloroform-*d*) δ 10.05 (s, 1H), 7.88-7.80 (m, 2H), 7.67 (p, *J* = 3.9 Hz, 1H), 4.29- 4.22 (m, 2H), 4.17 (d, *J* = 2.4 Hz, 2H), 3.78-3.70 (m, 4H), 3.55-3.49 (m, 4H), 2.49 (t, *J* = 4.9 Hz, 4H), 2.43 (t, *J* = 2.4 Hz, 1H).

^{13}C NMR (126 MHz, $CDCl_3$) δ 193.55, 159.29, 155.17, 152.37, 137.51, 127.40, 120.38, 79.37, 74.76, 68.08, 64.36, 64.03, 58.26, 52.97, 43.66.

ESI-MS: m/z $[M+H]^+$ calcd: 332.15; found, 332.94.

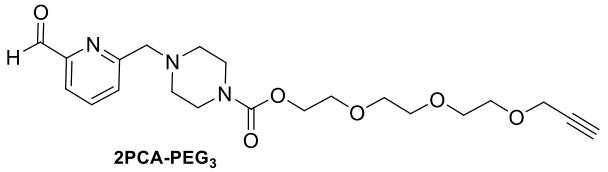

2PCA-PEG$_3$

^{1}H NMR (500 MHz, Chloroform-*d*) δ 10.06 (s, 1H), 7.88-7.83 (m, 2H), 7.69 (dd, *J* = 5.1, 3.8 Hz, 1H), 4.26-4.16 (m, 4H), 3.77 (s, 2H), 3.73-3.64 (m, 6H), 3.65 (s, 4H), 3.52 (s, 3H), 3.52 (d, *J* = 10.2 Hz, 2H), 2.50 (t, *J* = 5.0 Hz, 5H), 2.42 (t, *J* = 2.4 Hz, 1H), 2.00 (s, 2H).

^{13}C NMR (126 MHz, $CDCl_3$) δ 193.67, 159.43, 155.41, 152.51, 137.64, 127.53, 120.53, 79.73, 77.36, 74.71, 70.74, 70.65, 70.57, 69.72, 69.23, 64.73, 64.16, 58.54, 53.11, 43.84.

ESI-HRMS: m/z $[M+H]^+$ calcd: 420.2129; found, 420.2128.

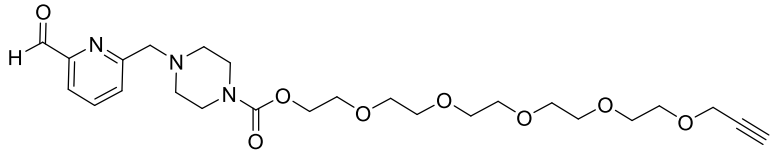

2PCA-PEG$_5$

^{1}H NMR (500 MHz, Chloroform-*d*) δ 10.06 (s, 1H), 7.88-7.83 (m, 2H), 7.68 (p, *J* = 3.9 Hz, 1H), 4.26-4.16 (m, 4H), 3.77 (s, 2H), 3.73-3.61 (m, 18H), 3.55-3.49 (m, 4H), 2.50 (t, *J* = 5.0 Hz, 4H), 2.42 (t, *J* = 2.4 Hz, 1H).

^{13}C NMR (126 MHz, $CDCl_3$) δ 193.57, 159.33, 155.27, 152.39, 137.51, 127.40, 120.39, 79.66, 76.80, 74.57, 70.61, 70.59, 70.57, 70.53, 70.41, 69.60, 69.11, 64.60, 64.06, 58.41, 53.00.

ESI-HRMS: m/z $[M+H]^+$ calcd: 508.2651; found, 508.2653.

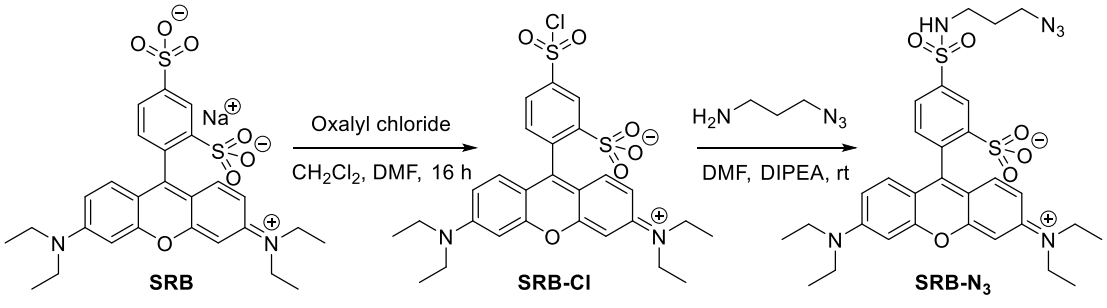

Scheme S2. Synthesis of **SRB-N$_3$**.

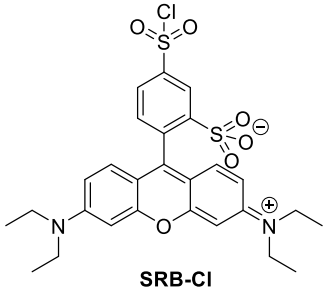

SRB-Cl

SRB-Cl was synthesized according to the literature.[S2] Briefly, to a stirred solution of sulforhodamine B sodium salt (**SRB**, 580 mg, 1 mmol) in CH_2Cl_2 (25 mL) at 0 °C, was sequentially added oxalyl chloride (430

μL, 5 mmol) slowly and a catalytic amount of anhydrous DMF (12 μL). The resulting mixture was stirred at room temperature for 16 h, and then the reaction was concentrated in vacuo and dried under vacuum to give **SRB-C**l (500 mg, 86.8%).

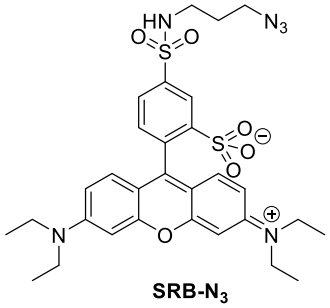

SRB-N$_3$

SRB-Cl (300 mg, 0.520 mmol) was dissolved in dry DMF (5 mL) under N_2. 3-Azidopropylamine (74.9 mg, 0.740 mmol) and DIPEA (121 mg, 0.940 mmol, 155 μL) were added and the reaction mixture was stirred overnight. Finally, the solvent was removed in vacuo and the crude product was purified by column chromatography (CH_2Cl_2/MeOH = 15/1). Yield: 60%.

^{1}H NMR (500 MHz, DMSO-d_6) δ 8.42 (d, *J* = 2.0 Hz, 1H), 8.03 (t, *J* = 5.9 Hz, 1H), 7.95 (dd, *J* = 7.9, 2.0 Hz, 1H), 7.49 (d, *J* = 7.9 Hz, 1H), 7.05 (dd, *J* = 9.6, 2.4 Hz, 2H), 7.01-6.93 (m, 4H), 5.77 (s, 1H), 3.71-3.59 (m, 8H), 3.41 (q, *J* = 14.0, 10.4 Hz, 3H), 2.94 (q, *J* = 6.6 Hz, 2H), 1.71 (q, *J* = 6.8 Hz, 2H), 1.21 (t, *J* = 7.0 Hz, 13H).

^{13}C NMR (126 MHz, DMSO) δ 157.89, 157.59, 155.50, 148.55, 141.79, 133.59, 133.15, 131.17, 126.17, 114.12, 113.94, 95.86, 55.39, 48.36, 45.73, 40.57, 40.48, 40.40, 40.31, 40.24, 40.14, 40.07, 28.97, 12.93.

ESI-HRMS: m/z $[M+H]^+$ calcd: 641.2208; found, 641.2209.

III. Molecular dynamics (MD) simulation

1. Initial structures and system preparations

The crystal structures of necitumumab (PDB ID: 6B3S) and cetuximab (PDB ID: 1YY9) were obtained directly from the PDB database.

Amino acid sequences for these two proteins were shown below with their N-terminal amino acids highlighted in red.

(1) Necitumumab Fab

>6B3S_2|Chains B[auth C], E[auth F], H, K[auth J]|**Necitumumab Fab Heavy chain**|Homo sapiens (9606)

QVQLQESGPGLVKPSQTLSLTCTVSGGSISSGDYYWSWIRQPPGKGLEWIGYIYYSGSTDYNPSLKS
RVTMSVDTSKNQFSLKVNSVTAADTAVYYCARVSIFGVGTFDYWGQGTLVTVSSASTKGPSVFPLA
PSSKSTSGTAALGCLVKDYFPEPVTVSWNSGALTSGVHTFPAVLQSSGLYSLSSVVTVPSSSLGTQTY
ICNVNHKPSNTKVDKKVEPKS

>6B3S_3|Chains C[auth D], F[auth G], I[auth K], L|**Necitumumab Fab Light chain**|Homo sapiens (9606)

EIVMTQSPATLSLSPGERATLSCRASQSVSSYLAWYQQKPGQAPRLLIYDASNRATGIPARFSGSGSG
TDFTLTISSLEPEDFAVYYCHQYGSTPLTFGGGTKAEIKRTVAAPSVFIFPPSDEQLKSGTASVVCLLN
NFYPREAKVQWKVDNALQSGNSQESVTEQDSKDSTYSLSSTLTLSKADYEKHKVYACEVTHQGLS
SPVTKSFNRGA

(2) Cetuximab Fab

>1YY9_2|Chain B[auth C]|**Cetuximab Fab Light chain**|Mus musculus (10090)

DILLTQSPVILSVSPGERVSFSCRASQSIGTNIHWYQQRTNGSPRLLIKYASESISGIPSRFSGSGSGTDF
TLSINSVESEDIADYYCQQNNNWPTTFGAGTKLELKRTVAAPSVFIFPPSDEQLKSGTASVVCLLNN
FYPREAKVQWKVDNALQSGNSQESVTEQDSKDSTYSLSSTLTLSKADYEKHKVYACEVTHQGLSS
PVTKSFNRGA

>1YY9_3|Chain C[auth D]|**Cetuximab Fab Heavy chain**|Mus musculus (10090)

QVQLKQSGPGLVQPSQSLSITCTVSGFSLTNYGVHWVRQSPGKGLEWLGVIWSGGNTDYNTPFTS
RLSINKDNSKSQVFFKMNSLQSNDTAIYYCARALTYYDYEFAYWGQGTLVTVSAASTKGPSVFPLA
PSSKSTSGGTAALGCLVKDYFPEPVTVSWNSGALTSGVHTFPAVLQSSGLYSLSSVVTVPSSSLGTQT
YICNVNHKPSNTKVDKRVEPKS

These two proteins were firstly pretreated by the Protein Preparation Wizard module[S3] of Schrödinger 2017-4 software (Schrödinger, LLC, New York) including the removal of all unbonded heteroatoms and water molecules, the replacement of missing hydrogen atoms, side chains, the use of the OPLS3 force field[S4] and the optimization of the structure to mitigate spatial collisions. Four small molecules, **P_nSRB** (the click conjugate of **2PCA-PEG$_n$** and **SRB-N$_3$**), where n = 1, 3, 5 and 7, respectively, were processed by Ligprep module[S5], and the protonated state was generated at pH = 7.0 ± 2.0. Then, by attaching small molecules to

the N-terminal of the light and heavy chains of proteins, respectively, we got eight complexes of small molecules and proteins as our initial structures.

2. Conventional molecular dynamics (MD) simulation

The antechamber and tleap tools in Amber16[S6] were used to prepare the initial molecular simulations of eight complexes. The AM1-BCC method[S7] (AM1 with bond charge corrections) was used to derive the partial charges of small molecules because of its relatively high computational speed and good performance in binding free energy calculations. The ff14SB[S8] and general Amber force field[S9] (gaff, version2.1) were employed to parameterize the proteins and small molecules, respectively. Each complex was immersed into a periodic truncated octahedral box filled with the TIP3P water molecules,[S10] and all the solute atoms were at least 10 Å away from the boundary of the water box. Then, counterions of Na^+ or Cl^- were added to neutralize the charge of each system. A hybrid protocol of the steepest descent method and the conjugate gradient method were employed to do the minimization. Ten-thousand steps of steepest descent minimization with the restraint (a force constant of 100 kcal/mol·$Å^2$) on the protein and ligand were first performed, and then the conjugate gradient method without any restraint was used until a maximum 20000 iteration steps was reached or the convergence criterion (the root-mean-square of the energy gradient is less than 1.0×10^{-4} kcal/mol·Å) was satisfied. The systems were heated up from 0 to 300 K linearly over a time period of 100 ps with the restraint (force constant of 10 kcal/mol·$Å^2$) on the solute in the NVT ensemble, and then the systems were equilibrated without restraint for 1 ns with a Langevin thermostat[S11] in the NPT (P = 1 atm and T = 300 K) ensemble. Finally, the 5 ns production runs were carried out with CUDA-version Amber16 in the NPT (P = 1 atm and T = 300 K) ensemble. The SHAKE algorithm[S12] was used to restrain the covalent bonds between heavy atoms and hydrogen atoms, and the time step was set to 2 fs. The snapshots were saved every 10 ps[S13, 14].

3. Trajectory analysis

The MD trajectories were post-processed by the CPPTRAJ module in AMBER 16,[S15] including stripping water and counterions. Then VMD software (version1.9.3)[S16] was used to calculate the distance between the centroid of the xanthene in two SRBs as the simulation time (the default of the maximum distance between the centroids of the two aromatic rings in π-π stacking is 4.0 Å[S17]). Based on DBSCAN (Density-Based

Spatial Clustering of Applications with Noise) clustering algorithm,[S18] the representative structures were extracted from the stable trajectories and drawn by Pymol software (version2.1.0).

4. Results and discussion

In order to explore whether the conjugated SRBs in necitumumab and cetuximab will form π-π stacking, the distances between the centroid of the xanthene in SRBs were measured over the course of the MD simulations. As shown in Figure S1a, in necitumumab, the distances as a function of simulation time exhibit fluctuations greatly at the beginning, suggesting that the conformations of these four small molecules are unstable. Hence, the stable trajectories during the last 1 ns were used for the following analyses. The average values of the distances are 7.50 Å, 5.77 Å, 3.97 Å and 3.16 Å in the conjugates of necitumumab with **P_1SRB**, **P_3SRB**, **P_5SRB** and **P_7SRB**, respectively. The similar fluctuations of distances also occur in cetuximab (Figure S1b). It can be observed that the distances tend to converge during the last 1.5 ns of the MD simulations. The average values of the distances in the conjugates of cetuximab with **$P_{1/3/5/7}$SRB** are 6.26 Å, 6.45 Å, 3.68 Å, 3.03 Å. It is reported that the benzene-benzene dimer is in the face-to-face configuration with an optimized distance of 3.9 Å. When they are too close, Pauli repulsion will force them apart, while at a further distance (more than 5 Å) the intermolecular interaction will be too weak[S19]. Thus in both necitumumab and cetuximab, **P_5SRB** should be ideal to form stable π-π stacking. Subsequently, standard deviations (SDs) of distances were calculated. In the conjugates of necitumumab and **$P_{1/3/5/7}$SRB**, SDs are 0.41 Å, 0.20 Å, 0.17 Å and 0.37 Å, and for cetuximab, SDs are 0.43 Å, 0.35 Å, 0.32 Å and 0.25 Å, respectively. These SDs are all less than 0.5 Å and the dispersion of the distances between small molecules is all small. Finally, representative conformations of the complexes were extracted with average distances and their SDs shown (Figure S2).

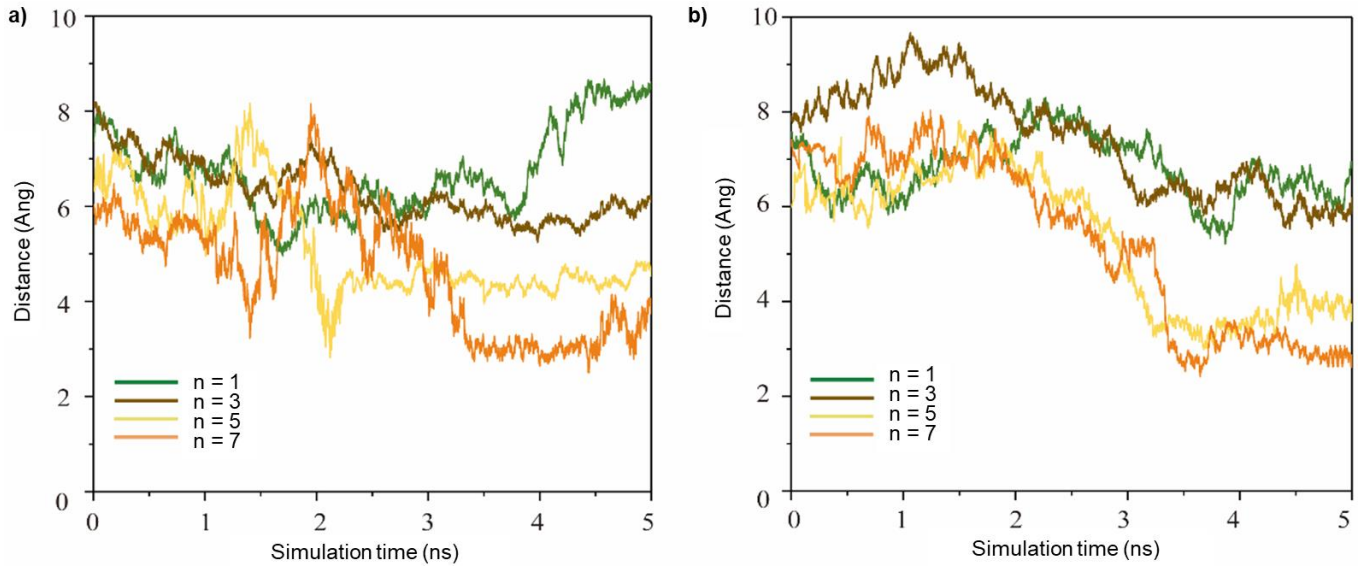

Figure S1. The distance between the centroid of the xanthene of two SRBs in a) **Nec-P$_n$SRB** and b) **Cet-P$_n$SRB** throughout the MD simulations.

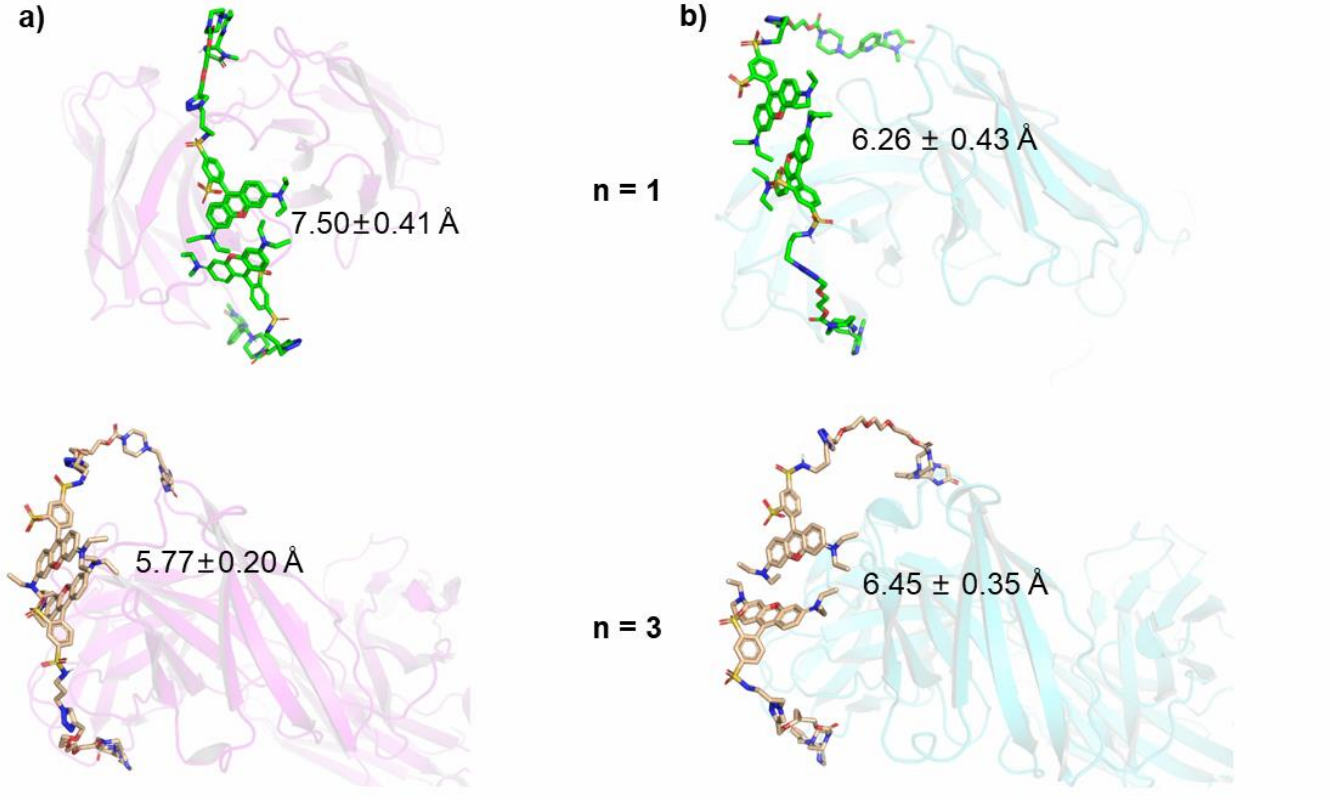

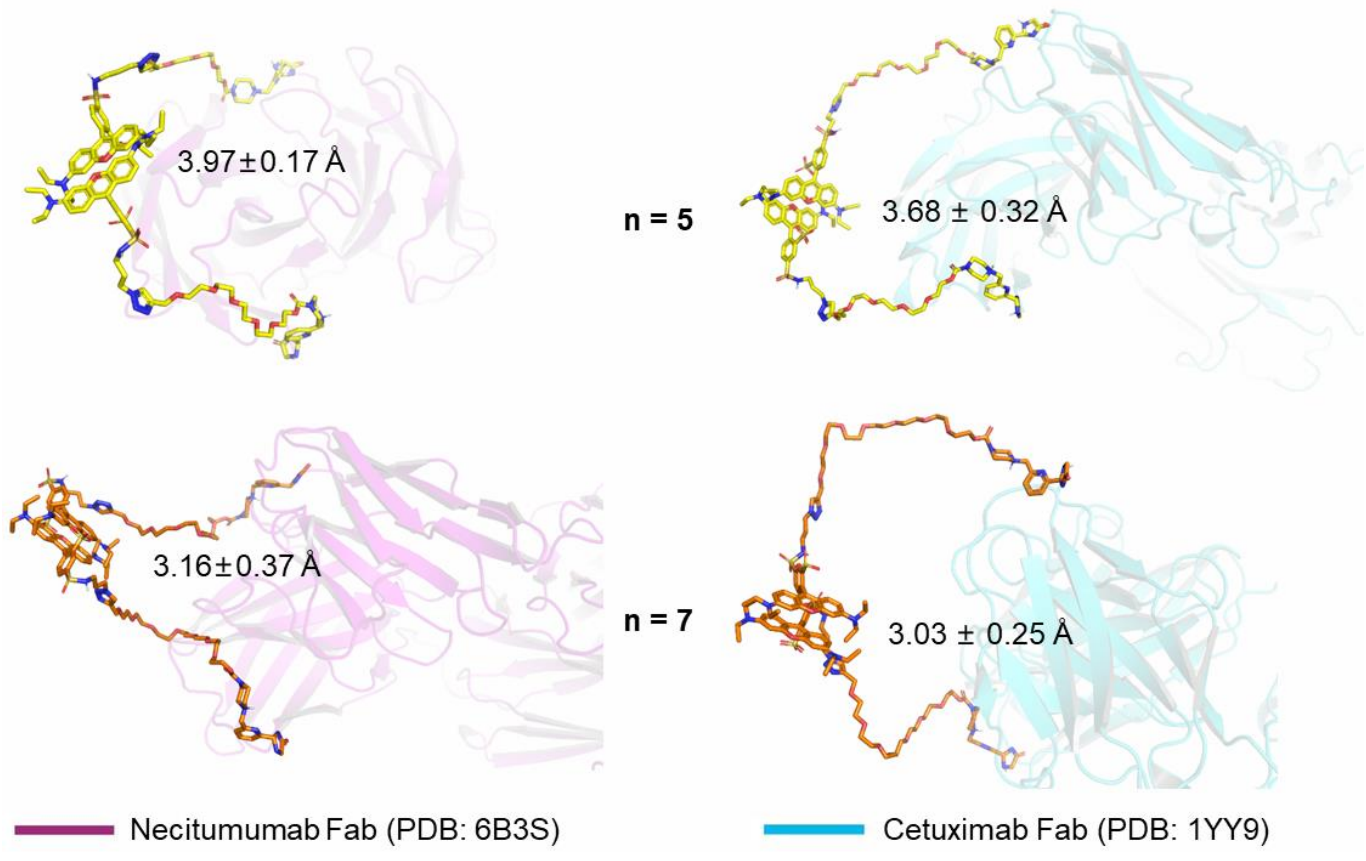

Figure S2. The representative conformations of a) **Nec-P$_n$SRB** and b) **Cet-P$_n$SRB** at the stable trajectories. The average distances between the centroid of the xanthene of two SRBs are listed.

IV. Antibody labeling and characterization

1. Modification procedures

Antibodies were chemically labeled using a previously reported procedure (Scheme S3)[S1]. Cetuximab/Necitumumab/IgG (20 μM, 950 μL) was reacted with 10 mM of **2PAC-PEG$_n$** in 50 mM phosphate buffer at pH 8.5 (a total volume of 1 mL). After 36 h at 37°C, excess **2PCA-PEG$_n$** was removed using a 12-14 kDa MWCO dialysis tubing. The resulting **Ab-PEG$_n$** (20 μM, 950 μL) was incubated with 120 μM of **SRB-N$_3$** for CuAAC/click chemistry (a mixture of 150 μM $CuSO_4$, 900 μM THPTA, 7.5 mM NaASc; in a total volume of 1 mL) for 12 h at room temperature. At the end, the antibodies were purified by Desalting Columns (17-0851-01 PD-10, GE Healthcare) against PBS (pH 7.5) to give the probe **Ab-P$_n$SRB**. To evaluate

the labeling efficiency, the conjugation was analyzed by 10% SDS-PAGE/in-gel fluorescence scanning (Figure S3).

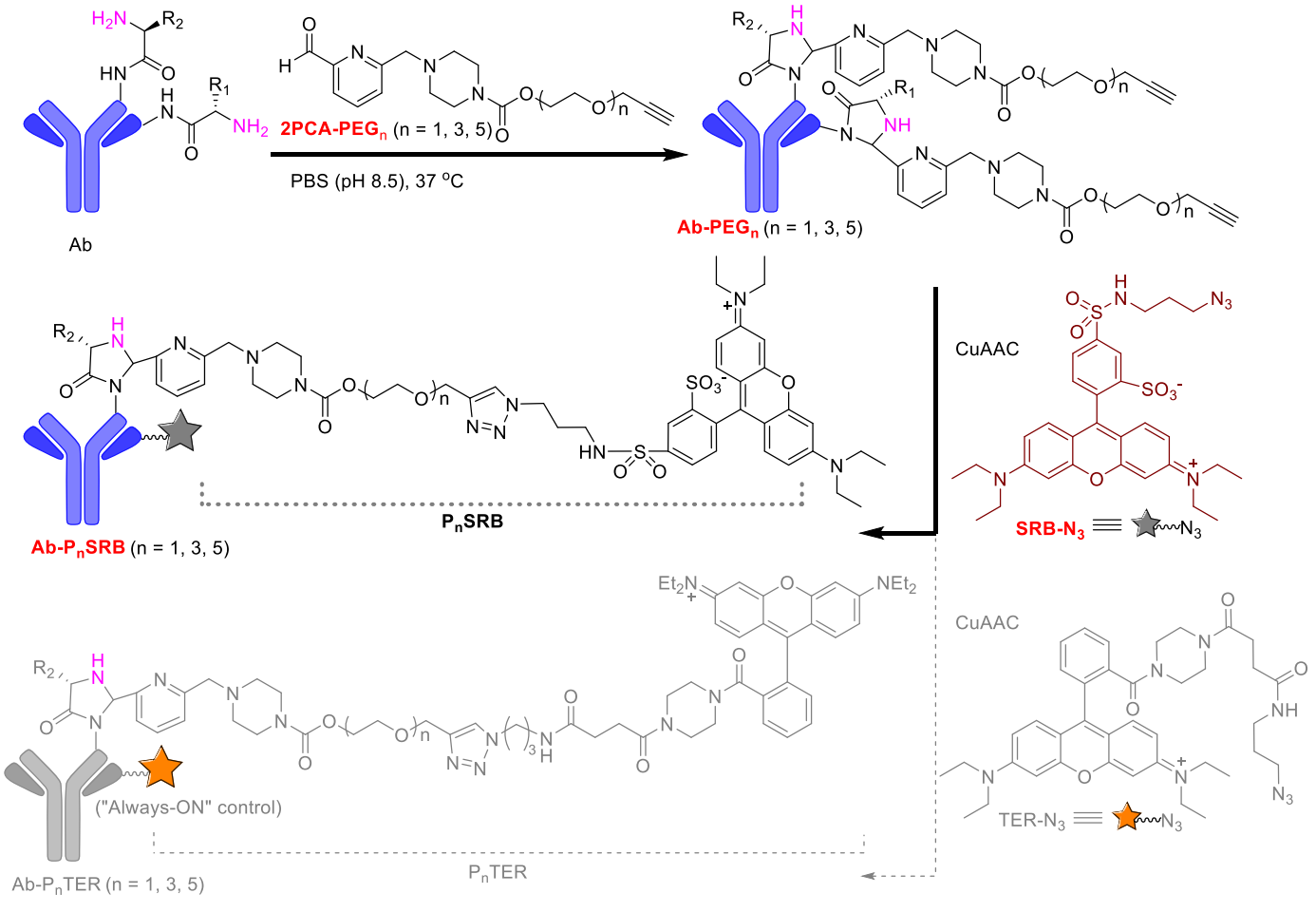

Scheme S3. Labeling of antibodies with **2PCA-PEG$_n$/SRB-N$_3$**. Ab may be Nec/Cet/IgG in this study. To simplify the illustration, the labeling is shown on one binding site here (there are two identical binding sites on each Y-shaped antibody). TER-N$_3$[S20], an "always-on" Rhodamine derivative, was used for comparison. CuAAC: copper(I)-catalyzed alkyne-azide cycloaddition.

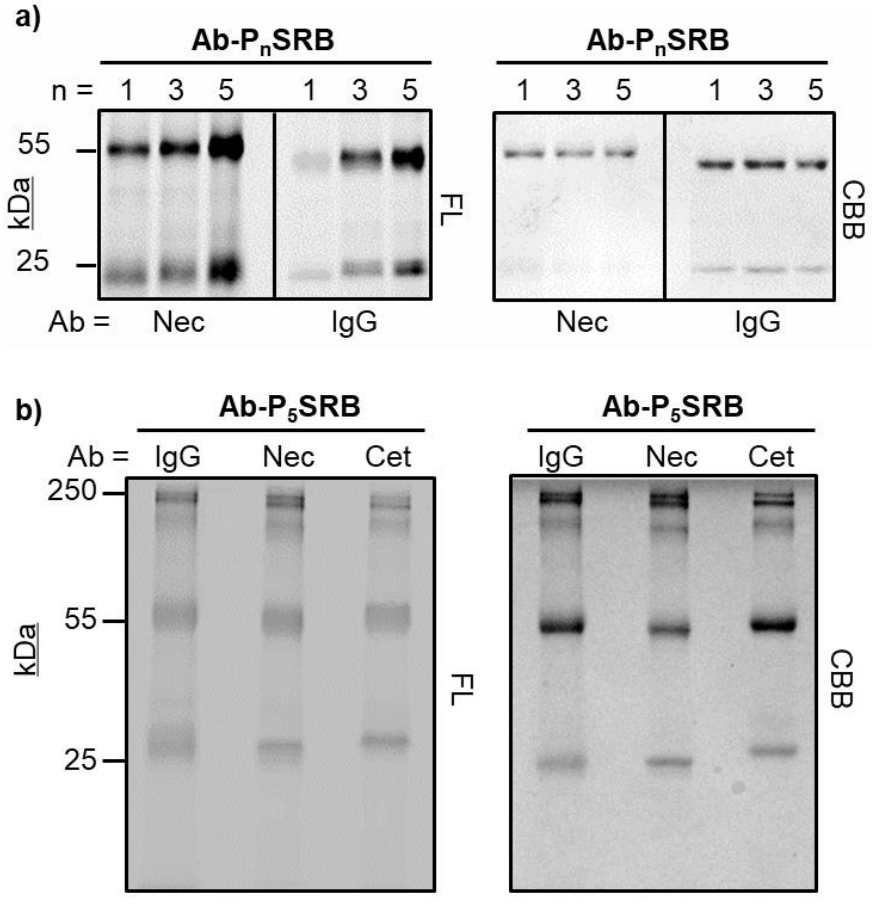

Figure S3. Labeling reactivity of a) **2PCA-PEG$_{1/3/5}$** (different in the PEG length) towards antibodies (i.e., necitumumab and IgG) and b) **2PCA-PEG$_5$** towards different antibodies, respectively, as visualized by in-gel fluorescent scanning (FL). Coomassie brilliant blue (CBB) staining showed the protein amount.

2. Quantitative analysis of **2PCA-PEG$_5$** labeling on antibody

The degree of **2PCA-PEG$_5$** labeling on antibodies was estimated following the reported procedure,[S21] by determining the Dye: Protein ratio of **Cet-PEG$_5$** and TER-N_3[S20] ("always-on" Rhodamine derivative; structure shown in Scheme S3) conjugate (Cet-P_5TER).

Table S1. Determination of Dye: Protein ratio in Cet-P_5TER conjugate.

	Cet-P_5TER conjugate
A_{280}	0.040
ε_{Ab}	174000 $M^{-1}cm^{-1}$

CF	0.2182
A_{max}	0.009
c_{Ab}	0.218 μM
ε_{dye}	55000 $M^{-1}cm^{-1}$
c_{dye}	0.164 μM
% of labeling	75%

(1) Calculate concentration of the antibody:

ε_{Ab} = 174000 $M^{-1}cm^{-1}$ for cetuximab[S22]

The correction factor (CF) equals the $A_{280\ (TER)}$ of the dye divided by the $A_{max\ (TER)}$ of the dye.

For TER-N_3:

$$A_{280\ (TER)} = 0.012$$

$$A_{560\ (TER)} = 0.055$$

$$CF = \frac{A_{280\ (TER)}}{A_{560\ (TER)}} = \frac{0.012}{0.055} = 0.2182$$

$$\text{Antibody concentration } (c_{Ab}) = \frac{A_{280}(0.040) - \left(A_{max}(0.009) \times CF\ (0.2182)\right)}{\varepsilon_{Ab}\ (174000)}$$

$$= 0.218\ \mu M$$

(2) Calculate the degree of labeling:

The maximum absorption of 1 μM dye detected in 1-cm standard quartz cells at 560 nm is 0.055, the molar absorption coefficient of dye (ε_{dye}) is 55000 $M^{-1}cm^{-1}$.

$$\text{Dye concentration } (c_{Dye}) = \frac{A_{max}(0.009)}{\varepsilon_{dye}\ (55000)} = 0.164\ \mu M$$

$$\%\text{ of labelled antibody} = \frac{c_{dye}}{c_{Ab}} = 75\%$$

3. <u>Evaluation of antigen binding with the modified antibodies</u>

Recombinant EGFR was mixed with 2×SDS-PAGE sample loading buffer (final concentration: 10 ng/μL) and 5 or 10 μL of the protein was separated on SDS-PAGE via a home-made 7.5% polyacrylamide gel and

transferred to PVDF membranes. Then 5% nonfat milk power solution was used for block followed by overnight incubation at 4 °C with **Nec-P_5SRB** and **Cex-P_5SRB** (100 ng in 4 mL) respectively. Unmodified necitumumab and cetuximab at the same concentration were used in parallel as control groups. Afterwards, the PVDF membrane was incubated with anti-human IgG (Fc gamma Fragment Specific) HRP-linked antibody (1:5000) for 2 hours at room temperature. The bands were visualized using enhanced chemiluminescence (ECL) regent under Imaging System (Azure biosystem) and analyzed by Image J 1.8 software.

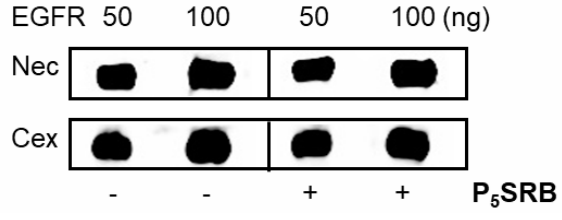

Figure S4. Retention of antigen binding ability of necitumumab and cetuximab before and after modification with **P_5SRB** as evaluated by western blotting analysis. 50 or 100 ng of recombinant EGFR (extracellular domain) was probed to the PVDF membrane followed by incubation with 100 ng of **P_5SRB** labeled or unlabeled necitumumab or cetuximab.

V. Determination of photophysical properties

1. Absorbance and fluorescence spectra scanning of small molecules

Absorbance spectra were recorded by TU-1801 ultraviolet-visible spectrophotometer (Beijing Purkinje General Instrument Co., Ltd.) and fluorescence spectra were recorded by HITACHI FL2700 steady-state fluorescence spectrophotometer (λ_{ex} = 530 nm). All samples were diluted in solvents as indicated and the measurements were performed in the 1-cm Micro quartz cell at room temperature.

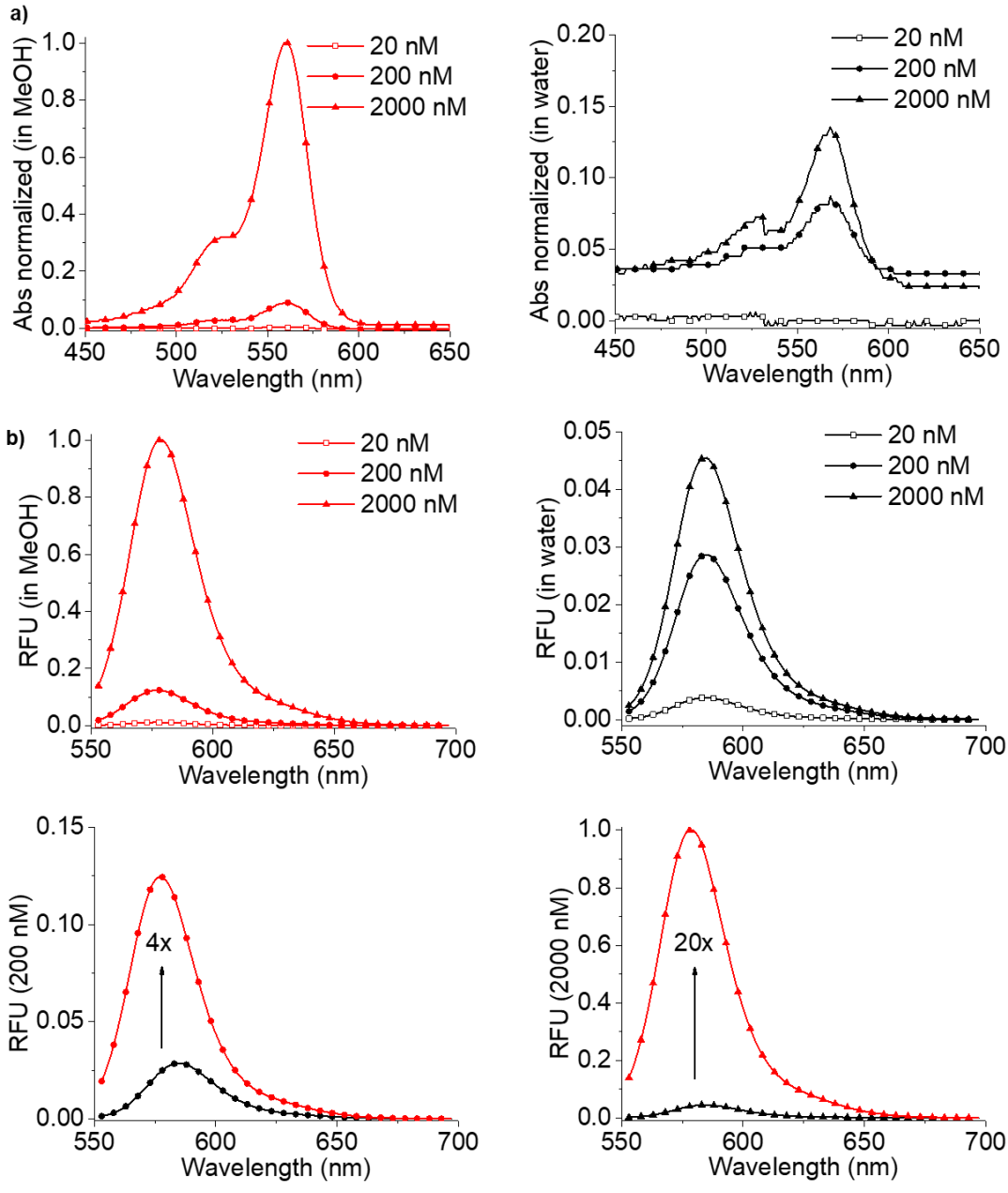

Figure S5. a) Absorbance and b) fluorescence spectra of **SRB-N$_3$** at different concentrations (20, 200, 2000 nM) in MeOH or water. Each set of data were independently normalized to the absorption and the emission maximum (set to 1) of 2000 nM **SRB-N$_3$** in a) and b), respectively.

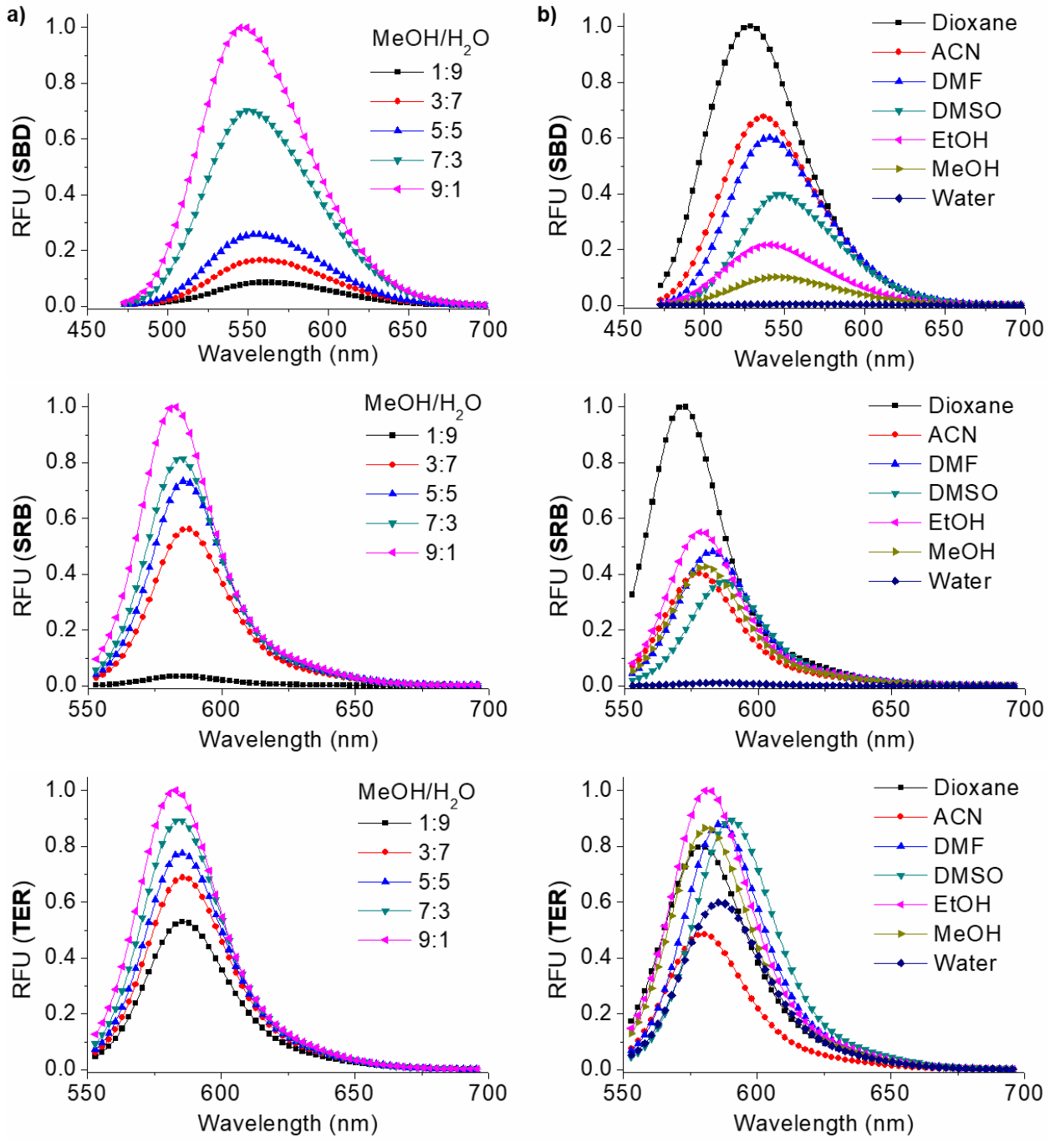

Figure S6. Fluorescence spectra of SBD (4-sulfamonyl-7-aminobenzoxadiazole)/**SRB-N$_3$**/TER-N$_3$ (5 μM) a) in MeOH-H_2O mixtures or b) in different solvents (λ_{ex} = 425 nm for SBD; λ_{ex} = 530 nm for **SRB-N$_3$** & TER-N$_3$). Increasing polarity: dioxane < DMF < DMSO < ACN < EtOH < MeOH < Water.[S23]

2. Absorbance and fluorescence spectra of **Ab-P$_n$SRB**

Comparison of absorbance (Figure S7a) and fluorescence (λ_{ex} = 530 nm; Figure 2b in main text) spectra of **Nec-P$_n$SRB** and **SRB-N$_3$** at room temperature as performed on BioTek Synergy H1FMG microplate reader. The fluorescence spectra of IgG-P$_5$TER and TER-N$_3$ (λ_{ex} = 530 nm) were also tested to check the difference between our **IgG-P$_5$SRB** and the "always-on" one (Figure S7b).

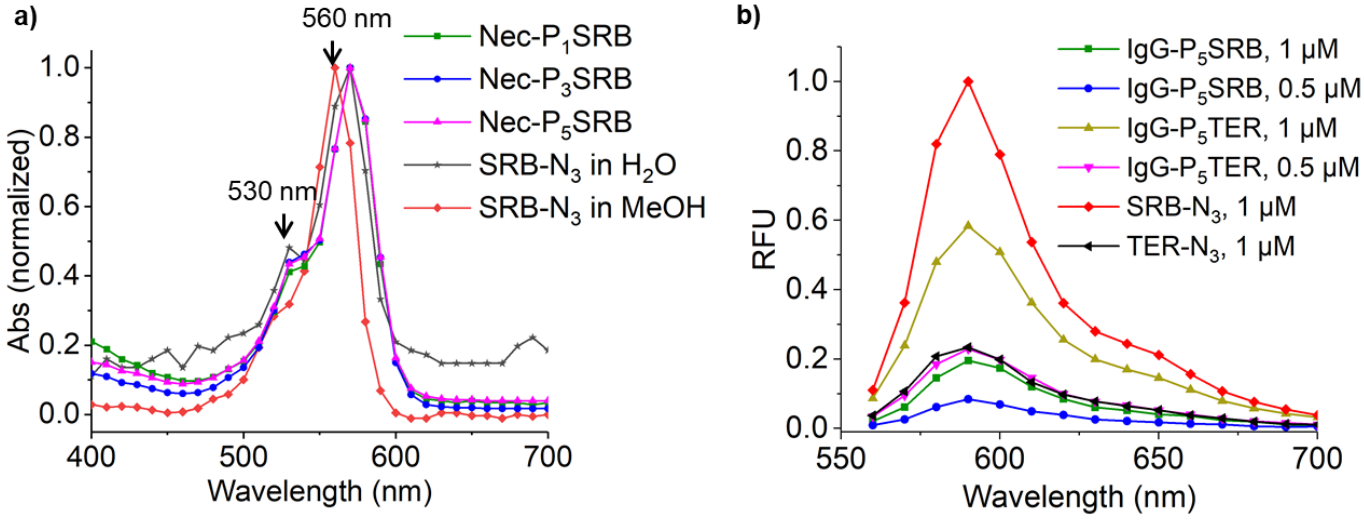

Figure S7. a) Absorbance spectra of **Nec-P$_{1/3/5}$SRB** (17 μM) and **SRB-N$_3$** (2 μM) in H_2O or MeOH after normalization (each set of data were independently normalized to the absorption maximum (set to 1)). b) Fluorescence spectra of **IgG-P$_5$SRB**, IgG-P$_5$TER, **SRB-N$_3$**, and TER-N$_3$ in H_2O (λ_{ex} = 530 nm).

3. Fluorescence response of **Ab-P$_5$SRB** towards recombinant EGFR

Comparison of fluorescence responses of **Nec-P$_5$SRB** and **IgG-P$_5$SRB** (20 nM, 97 μL) towards different ratios of recombinant EGFR (3 μL) in water after incubation for 30 min at room temperature was performed on BioTek Synergy H1FMG microplate reader (λ_{ex} = 560 nm, λ_{em} = 590 nm; Figure 2c in main text).

VI. Live-cell imaging

For confocal laser scanning microscope (CLSM) experiments, A431, A549 and HepG2 cells were cultured in Dulbecco's Modified Eagle's Medium (DMEM) supplemented with 10% fetal bovine serum (FBS), 100.0 mg/L streptomycin and 100 IU/mL penicillin in a humidified atmosphere of 5% CO_2 at 37 °C. Cells were seeded in a 4-chamber glass-bottom dish (D35C4-20-1-N, Cellvis) and grown until 50~60% confluency.

Upon medium removal, cells were washed once with DMEM and treated with **Ab-P$_n$SRB** at indicated concentrations in 250 μL DMEM. The cells were imaged without washing by the LSM 880, AxioObserver Confocal Microscope System (λ_{ex} = 561 nm, λ_{em} = 581-639 nm).

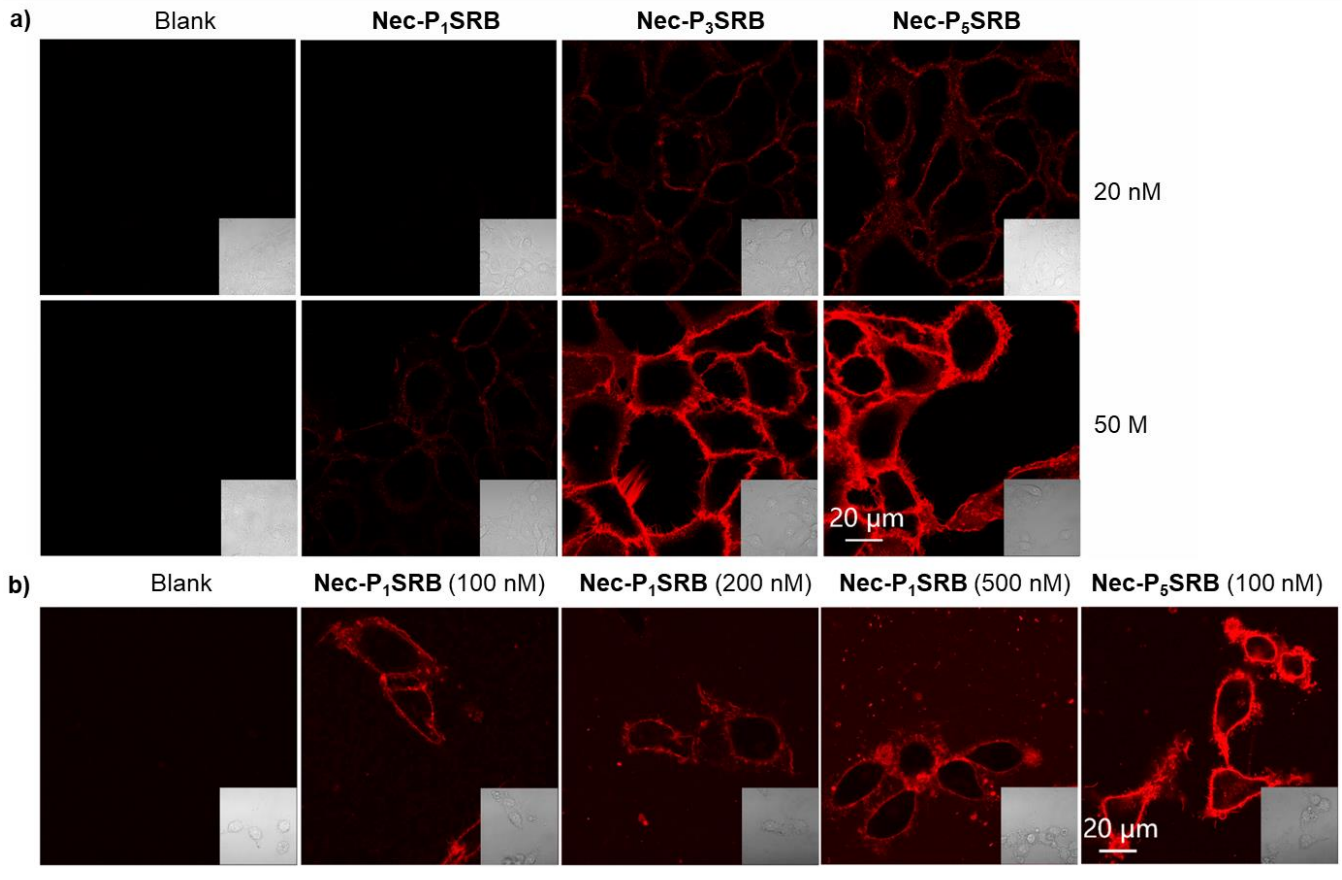

Figure S8. a) Live-cell imaging of A431 cells incubated with **Nec-P$_n$SRB** at 20 nM (up) or 50 nM (down) without washing. b) Wash-free live-cell imaging of A431 cells incubated with **Nec-P$_1$SRB** at 100, 200 or 500 nM as compared with cells using **Nec-P$_5$SRB** at 100 nM.

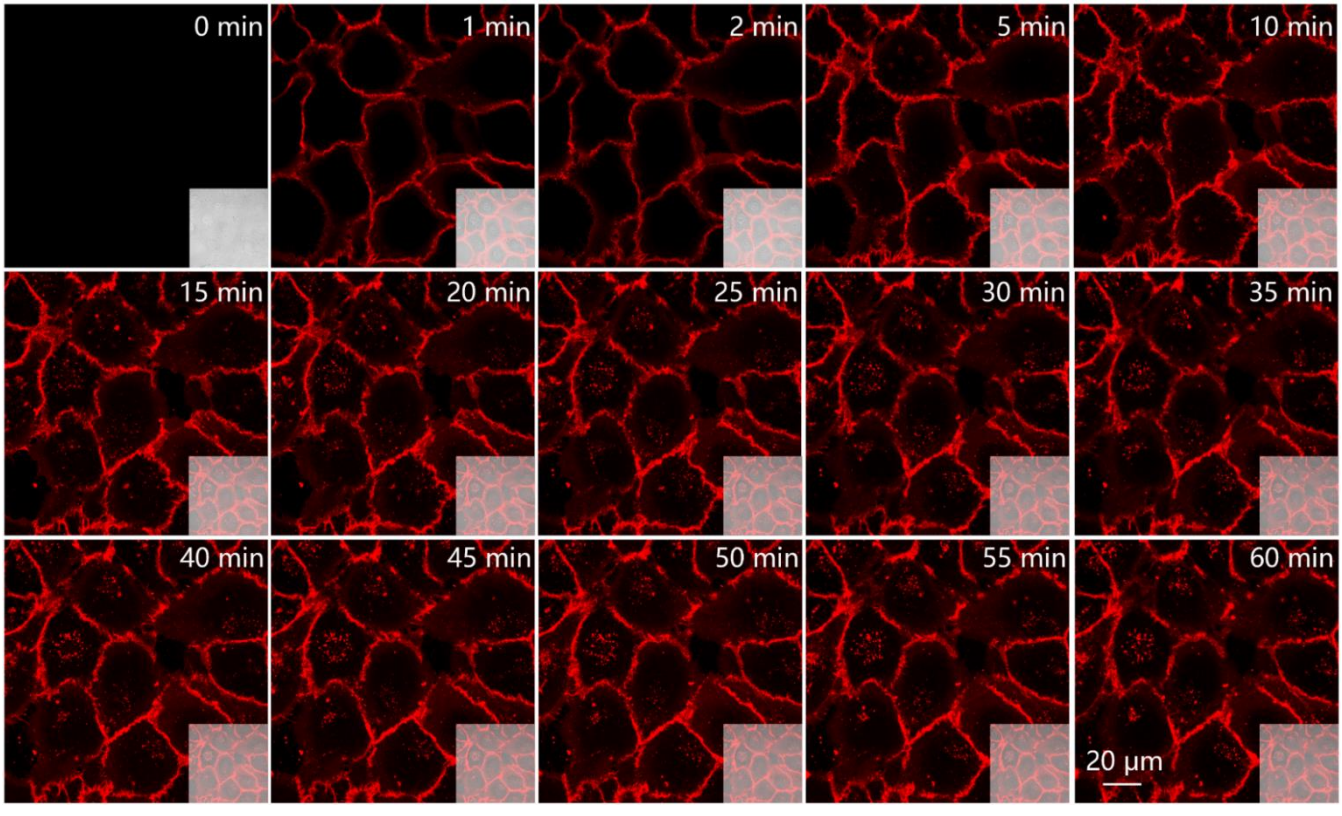

Figure S9. Real-time imaging of A431 cells upon addition of **Nec-P$_5$SRB** (100 nM).

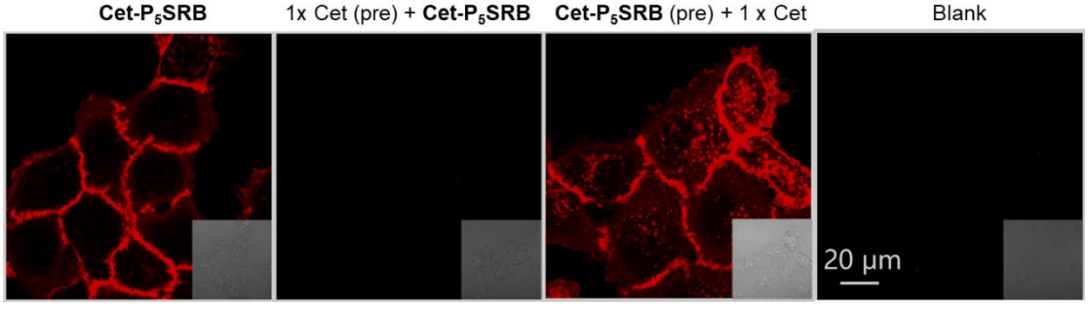

Figure S10. No-wash imaging of A431 cells by using **Cet-P$_5$SRB** (100 nM) with or without presence of the non-labelled cetuximab (100 nM). In the second panel, cells were pretreated (pre) with cetuximab for 0.5 h. After removal of cetuximab, cells were incubated with **Cet-P$_5$SRB** for 5 min before imaging. In the third panel, cells were pretreated (pre) with **Cet-P$_5$SRB** for 0.5 h. After removal of the probe, cells were incubated with cetuximab for 5 min before imaging.

VII. FACS[S24]

For FACS experiments, A431, A549 and HepG2 cells were seeded in a 12 plate (ExCell Biology) and cultured overnight. Upon medium removal, the cells were washed three times with PBS and treated with **Nec-P$_5$SRB** at indicated concentrations in 0.5 mL of DMEM. The cells were incubated for 10 min at 37 ^{o}C and washed three times with PBS. The resulting cells were detached from the plate by treatment with 200 μL of 0.1% trypsin-EDTA at 37 ^{o}C for 2 min. The detached cells were collected by centrifugation. Upon further washing with cold PBS (500 μL) three times, the cells were suspended in 300-500 μL of PBS. Cells were analyzed on a CytoFLEX LX cell analyzer (10,000 cells were counted for each event; in duplicate) using λ_{ex} = 561 nm, λ_{em} = 610 ± 20 nm (mCherry) for SRB.

Western blotting assay was carried out to determine the endogenous EGFR expression levels as reference for FACS. A431, A549, HEPG2 cells were seeded in 60-mm dishes and cultured to 70-80% confluence, the culture medium was removed and cells were washed with cold PBS for three times. Cells were lysed with RIPA lysis buffer and sonicated. The protein concentration of the supernatant was determined using BCA Protein Assay Kit (Beyotime Biotechnology, Shanghai, China) according to the kit instruction. Same amount of total proteins were loaded and separated on SDS-PAGE before transferred to PVDF membranes. After blocking by 5% nonfat milk power and incubating overnight with primary antibodies (1:1000) (EGF Receptor D381XP Rabbit mAb, Cell Signaling Technology) at 4 °C, horseradish peroxide-conjugated secondary antibody (1:5000, Goat anti-Rabbit IgG, Multi Sciences) was applied for 2 h at room temperature. The bands were visualized using ECL regent under BiosystemsAzure600.

VIII. References

S1. J. I. MacDonald, H. K. Munch, T. Moore and M. B. Francis, *Nat. Chem. Biol.* **2015**, *11*, 326-331.

S2. F. Bouhedda, K. T. Fam, M. Collot, A. Autour, S. Marzi, A. Klymchenko and M. Ryckelynck, *Nat. Chem. Biol*. **2020**, *16*, 69-76.

S3. G. M. Sastry, M. Adzhigirey, T. Day, R. Annabhimoju and W. Sherman, *J. Comput. Aid Mol. Des.* **2013**, *27*, 221-234.

S4. E. Harder, W. Damm, J. Maple, C. J. Wu, M. Reboul, J. Y. Xiang, L. L. Wang, D. Lupyan, M. K. Dahlgren, J. L. Knight, J. W. Kaus, D. S. Cerutti, G. Krilov, W. L. Jorgensen, R. Abel and R. A. Friesner, *J. Chem. Theory. Comput*. **2016**, *12*, 281-296.

S5. Z. Wang, X. W. Wang, Y. Kang, H. Y. Zhong, C. Shen, X. J. Yao, D. S. Cao and T. J. Hou, *Phys. Chem. Chem. Phys*. **2020**, *22*, 5487-5499.

S6. D. A. Case, T. E. Cheatham, T. Darden, H. Gohlke, R. Luo, K. M. Merz, A. Onufriev, C. Simmerling, B. Wang and R. J. Woods, *J. Comput. Chem*. **2005**, *26*, 1668-1688.

S7. M. Suruzhon, T. Senapathi, M. S. Bodnarchuk, R. Viner, I. D. Wall, C. B. Barnett, K. J. Naidoo and J. W. Essex, *J. Chem. Inf. Model*. **2020**, *60*, 1917-1921.

S8. J. A. Maier, C. Martinez, K. Kasavajhala, L. Wickstrom, K. E. Hauser and C. Simmerling, *J. Chem. Theory. Comput*. **2015**, *11*, 3696-3713.

S9. J. M. Wang, R. M. Wolf, J. W. Caldwell, P. A. Kollman and D. A. Case, *J. Comput. Chem*. **2004**, *25*, 1157-1174.

S10. D. Paschek, R. Day and A. E. Garcia, *Phys. Chem. Chem. Phys*. **2011**, *13*, 19840-19847.

S11. R. J. Loncharich, B. R. Brooks and R. W. Pastor, *Biopolymers* **1992**, *32*, 523-535.

S12. S. Miyamoto and P. A. Kollman, *J. Comput. Chem*. **1992**, ***13***, 952-962.

S13. N. Liu, W. F. Zhou, Y. Guo, J. M. Wang, W. T. Fu, H. Y. Sun, D. Liu, M. J. Duan and T. J. Hou, *J. Chem. Inf. Model*. **2018**, *58*, 1652-1661.

S14. Y. Jin, M. J. Duan, X. W. Wang, X. T. Kong, W. F. Zhou, H. Y. Sun, H. Liu, D. Li, H. D. Yu, Y. Y. Li and T. J. Hou, *J. Chem. Inf. Model*. **2019**, *59*, 842-857.

S15. D. A. Pearlman, D. A. Case, J. W. Caldwell, W. S. Ross, T. E. Cheatham, S. Debolt, D. Ferguson, G. Seibel and P. Kollman, *Comput. Phys. Commun*. **1995**, *91*, 1-41.

S16. W. Humphrey, A. Dalke and K. Schulten, *J. Mol. Graph. Model*. **1996**, *14*, 33-38.

S17. K. Carter-Fenk and J. M. Herbert, *Phys. Chem. Chem. Phys*. **2020**, *22*, 24870-24886.

S18. M. Ester, H. P. Kriegel, J. Sander and X. Xu, *KDD-96* **1996**, *96*, 226-231.

S19. R. D. Zhao and R. Q. Zhang, *Phys. Chem. Chem. Phys*. **2016**, *18*, 25452-25457.

S20. J. Y. Ge, C. W. Zhang, X. W. Ng, B. Peng, S. J. Pan, S. B. Du, D. Y. Wang, L. Li, K. L. Lim, T. Wohland and S. Q. Yao, *Angew. Chem. Int. Ed.* **2016**, *55*, 4933-4937.

S21. S. S. Liew, C. W. Zhang, J. Zhang, H. Y. Sun, L. Li and S. Q. Yao, *Chem. Commun*. **2020**, *56*, 11473-11476.

S22. X. J. Shi, C. Y. Y. Yu, H. F. Su, R. T. K. Kwok, M. J. Jiang, Z. K. He, J. W. Y. Lam and B. Z. Tang, *Chem. Sci*. **2017**, *8*, 7014-7024.

S23. http://murov.Info/orgsolvents.htm#TABLE%202

S24. L. H. Qian, J. Q. Fu, P. Y. Yuan, S. B. Du, W. Huang, L. Li and S. Q. Yao, *Angew. Chem. Int. Edit*. **2018**, *57*, 1532-1536.

IX. NMR and MS spectra

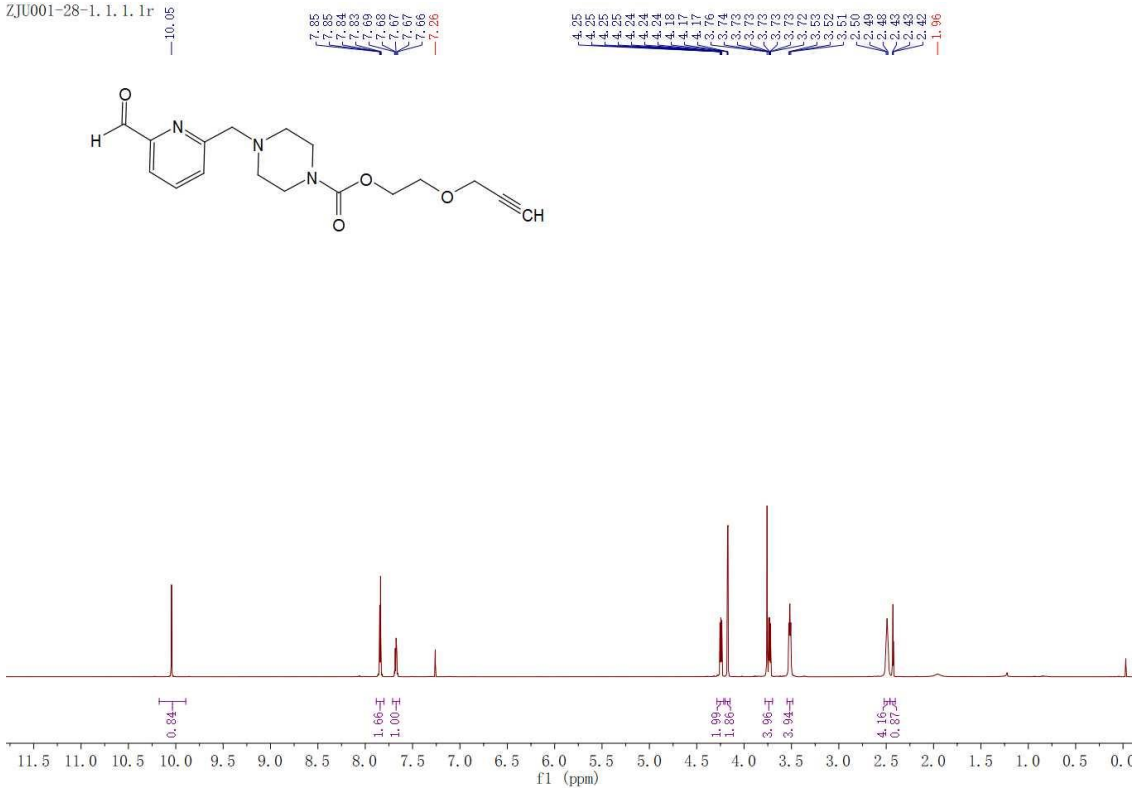

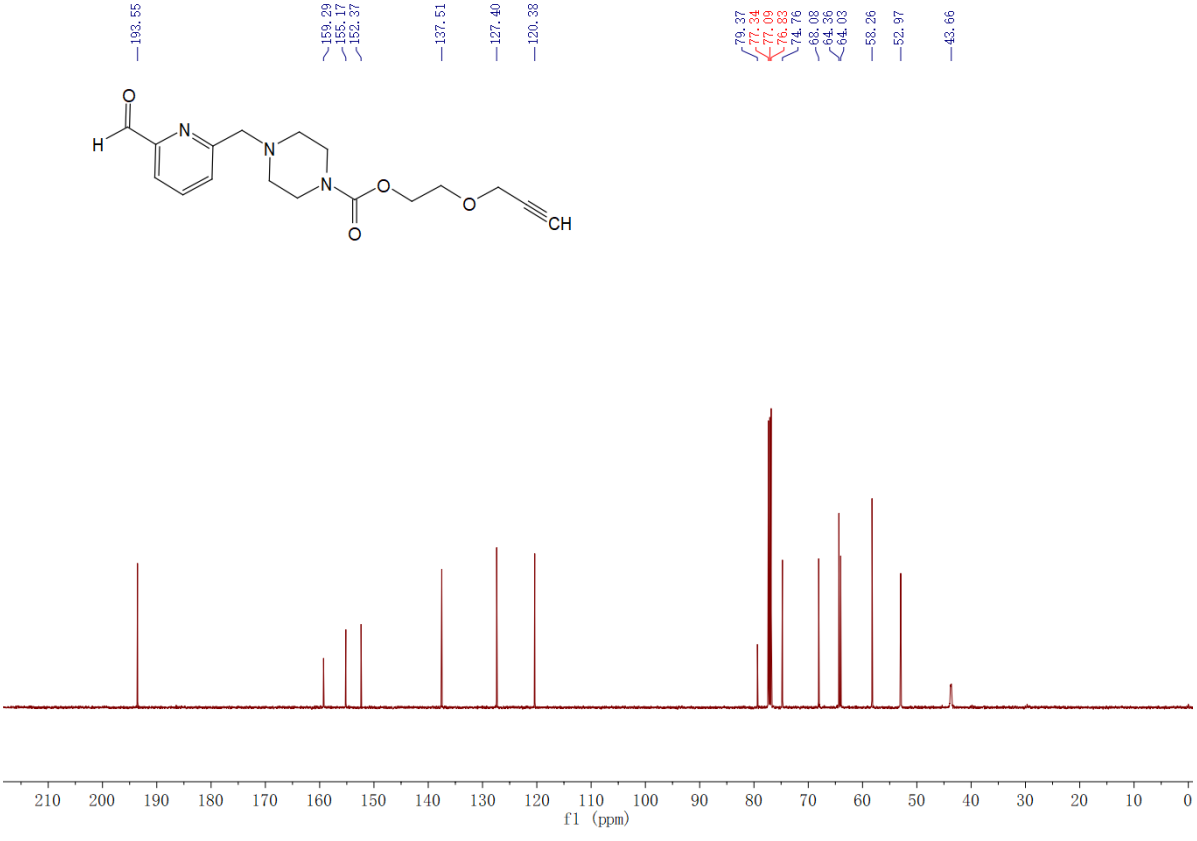

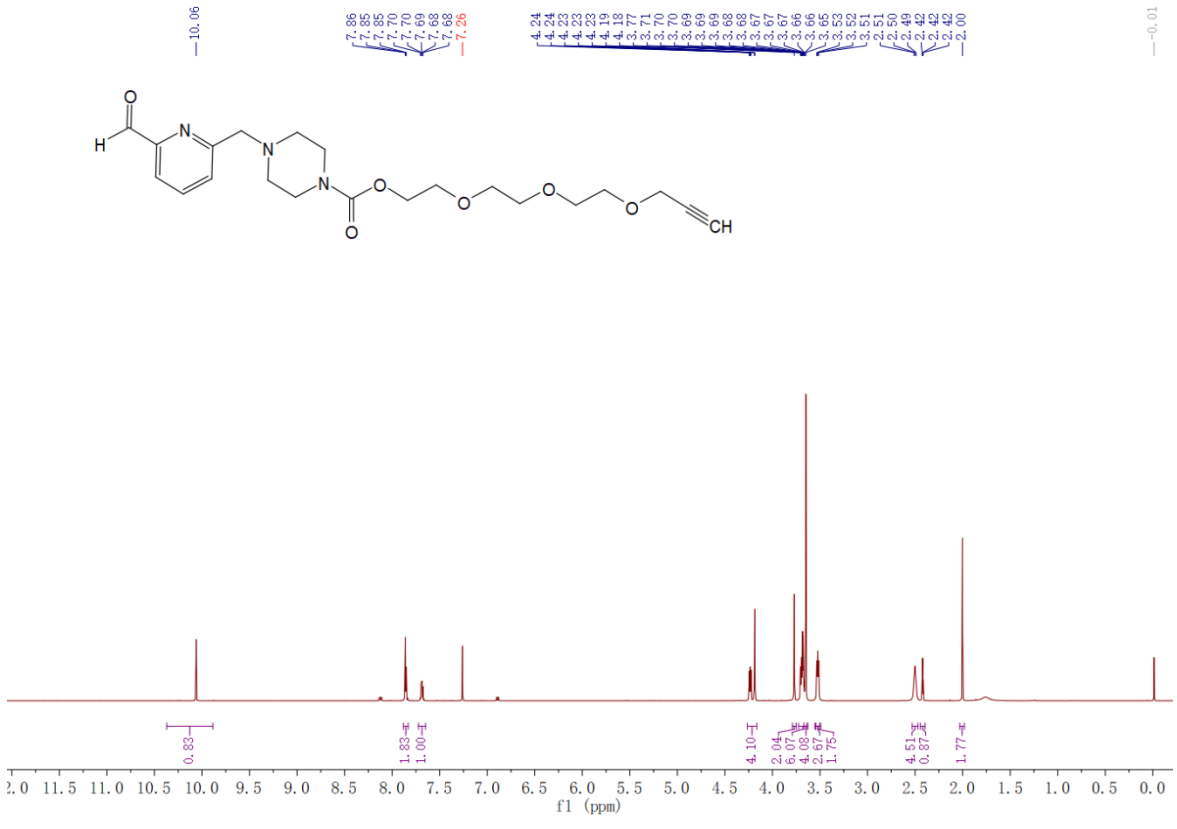
10.06
7.86
7.85
7.85
7.70
7.70
7.69
7.68
7.68
7.26
4.24
4.24
4.23
4.23
4.23
4.19
4.18
3.77
3.71
3.70
3.70
3.69
3.69
3.68
3.68
3.67
3.67
3.67
3.66
3.66
3.65
3.53
3.52
3.51
2.51
2.50
2.49
2.42
2.42
2.42
2.00
0.01
0.83
1.83
1.00
4.10
2.04
6.07
4.08
2.75
4.51
0.87
1.77
f1 (ppm)

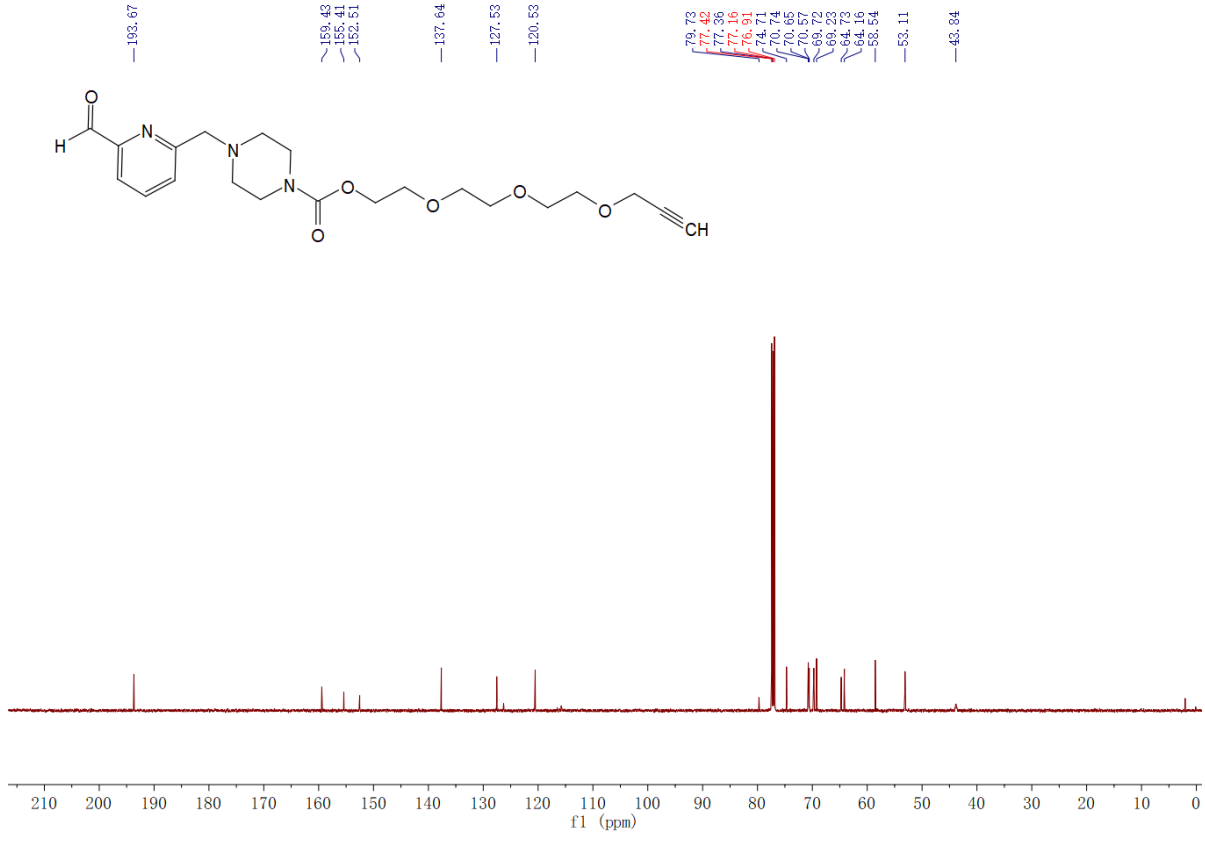
193.67
159.43
155.41
152.51
137.64
127.53
120.53
79.73
77.42
77.36
77.16
76.91
74.71
70.74
70.65
70.57
69.72
69.23
64.73
64.16
58.54
53.11
43.84
f1 (ppm)

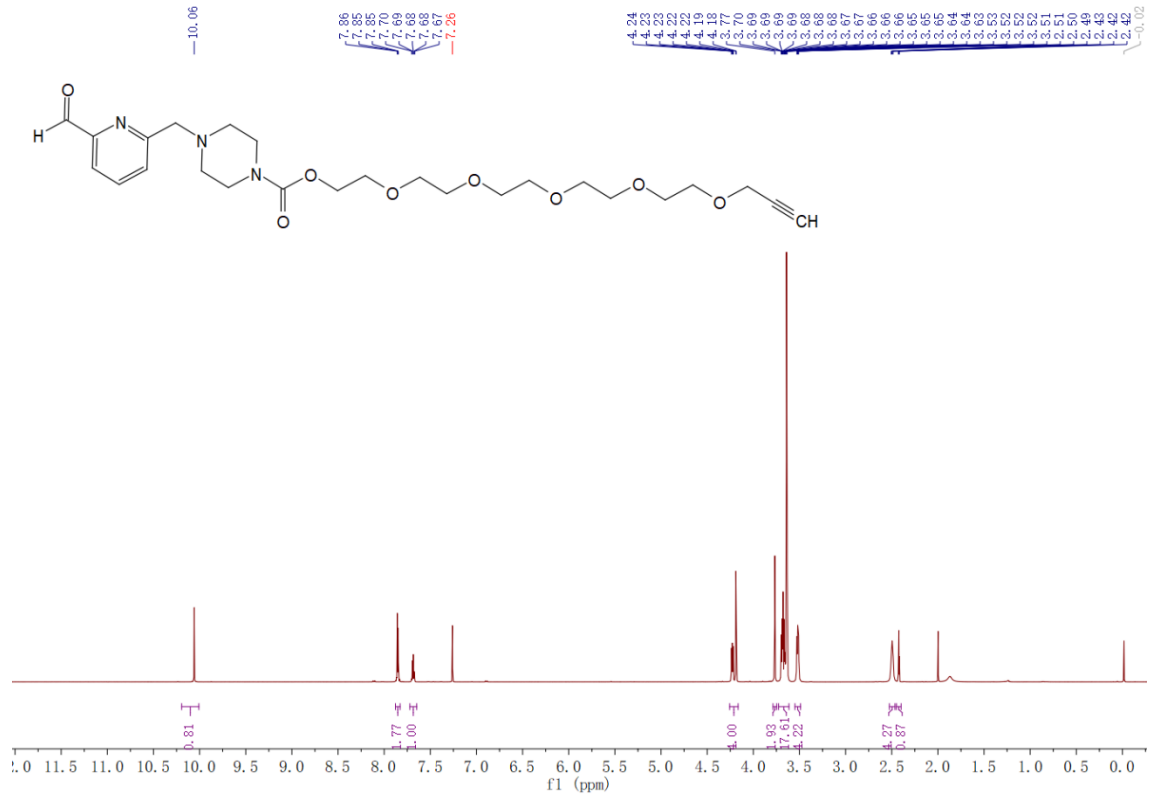
10.06
7.86
7.85
7.85
7.70
7.69
7.68
7.68
7.67
7.26
4.24
4.23
4.23
4.22
4.22
4.19
4.18
3.77
3.70
3.69
3.69
3.69
3.68
3.68
3.68
3.67
3.67
3.66
3.66
3.66
3.65
3.65
3.64
3.64
3.64
3.63
3.53
3.52
3.52
3.52
3.51
3.51
2.50
2.49
2.43
2.42
2.42
0.02
0.81
1.77
1.00
4.00
1.93
17.61
4.22
4.27
0.87
f1 (ppm)

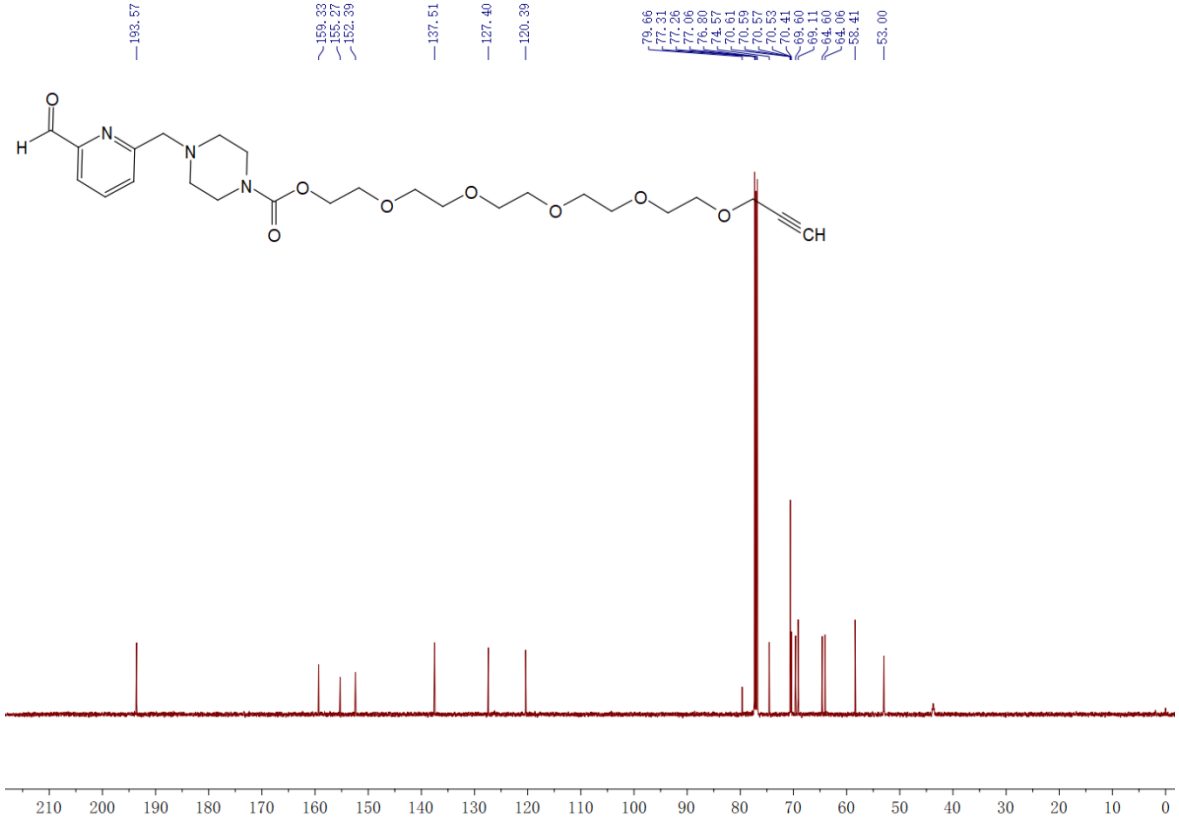
193.57
159.33
155.27
152.39
137.51
127.40
120.39
79.66
77.31
77.26
77.06
76.80
74.57
70.61
70.59
70.57
70.53
70.41
69.60
69.11
64.60
64.06
58.41
53.00

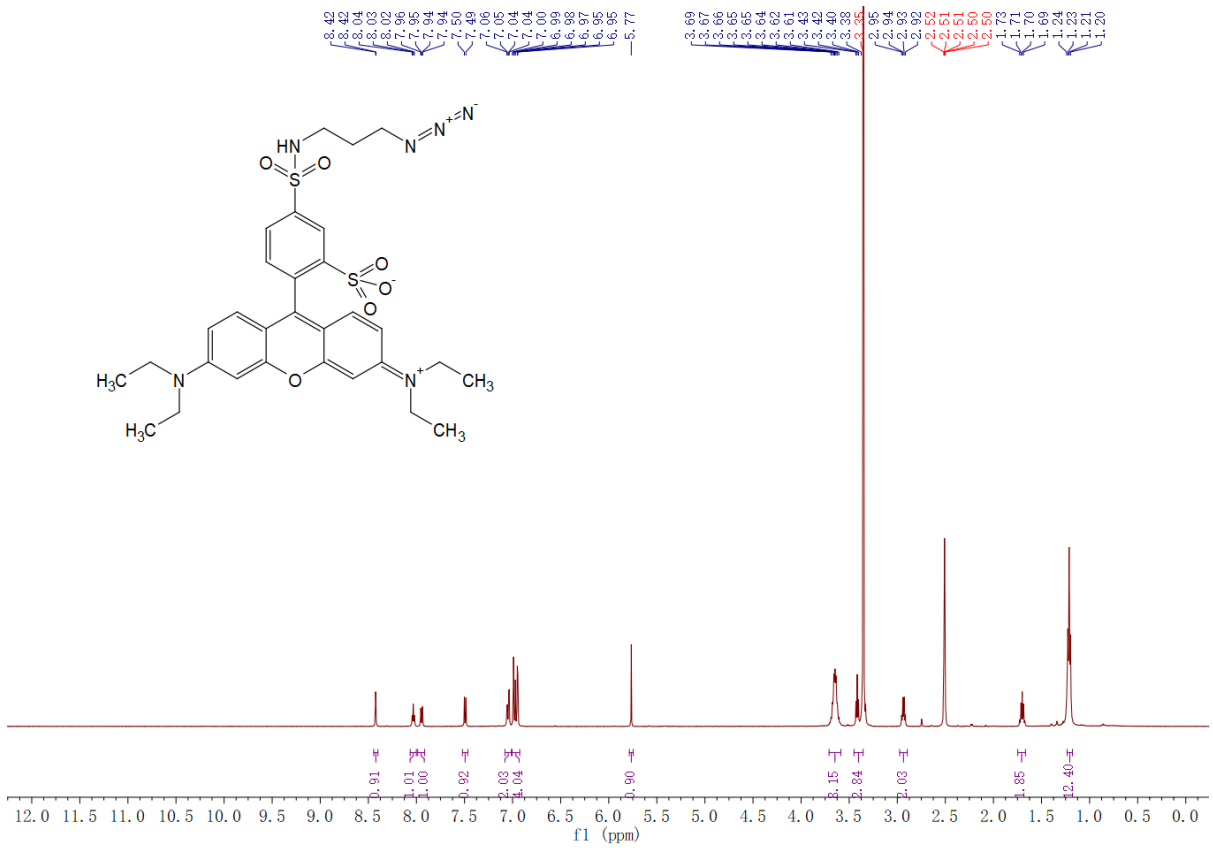
f1 (ppm)

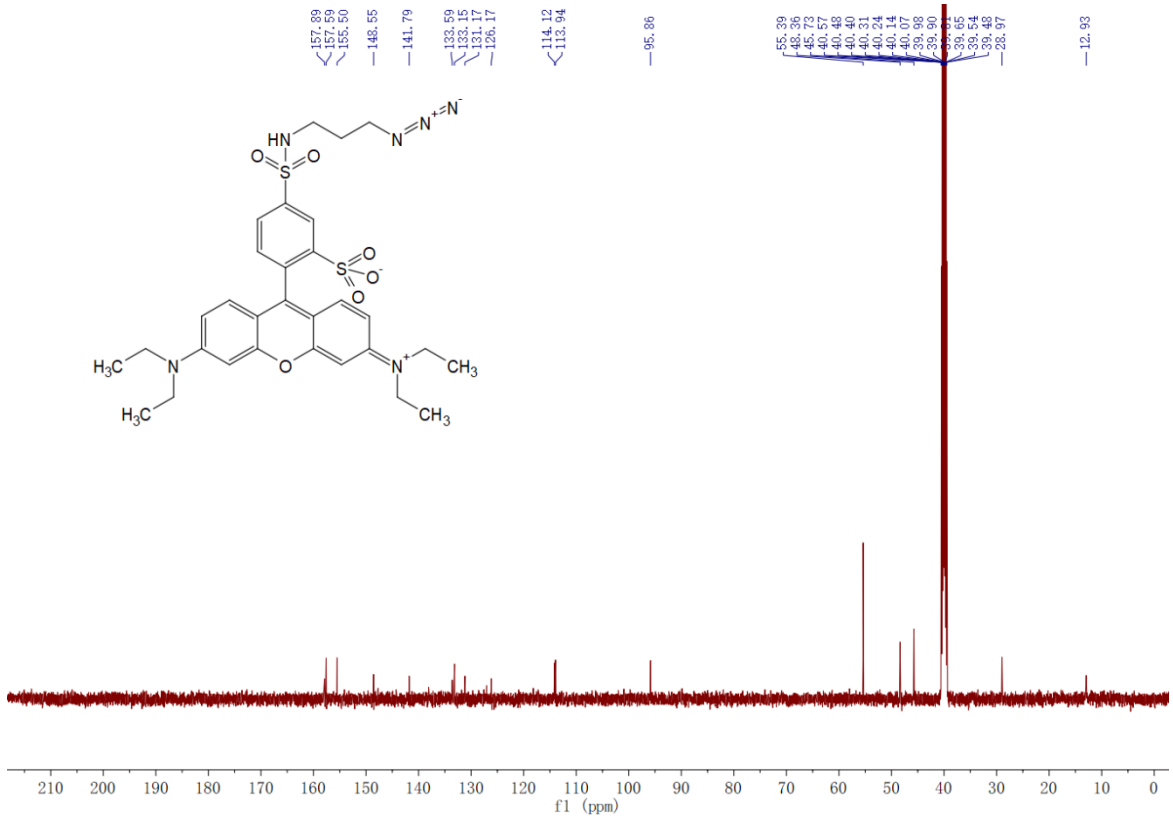
f1 (ppm)

(1) ESI-MS for **2PCA-PEG$_1$**

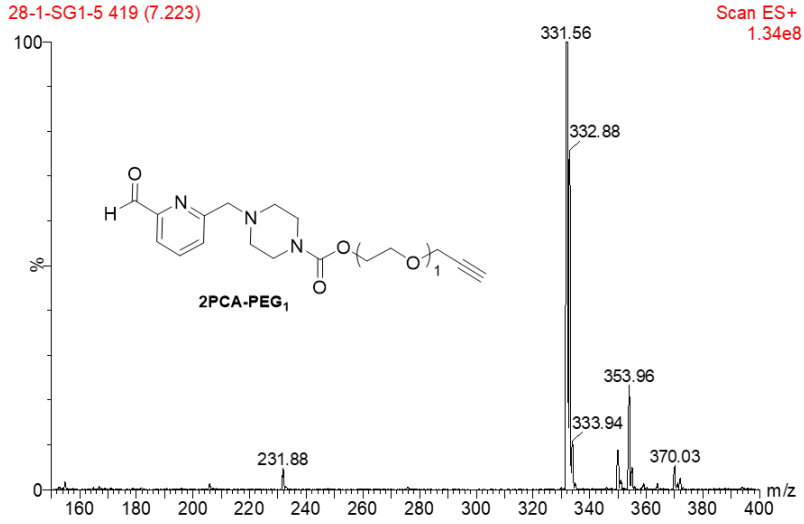

(2) ESI-HRMS for **2PCA-PEG$_3$**

Spectra

Fragmentor Voltage	Collision Energy	Ionization Mode
100	0	ESI

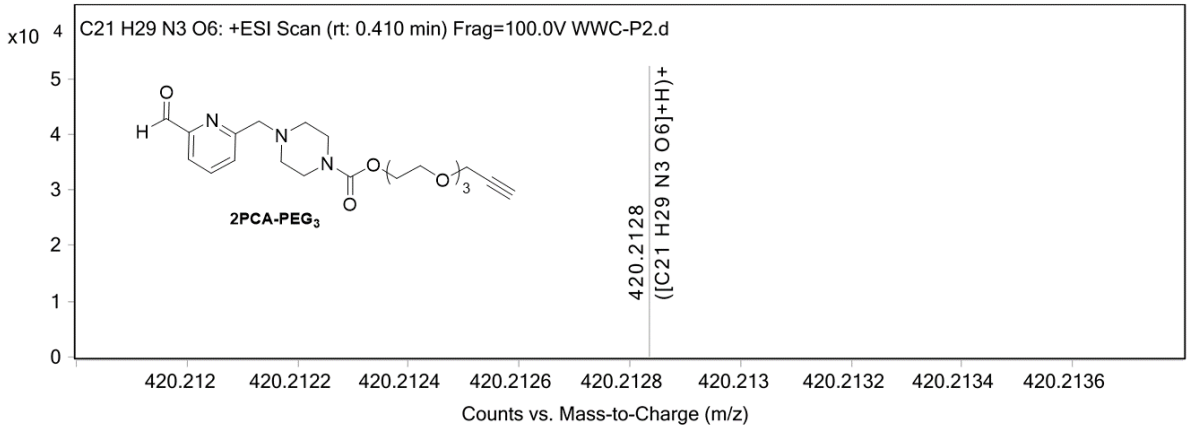

Formula Calculator Element Limits

Element	Min	Max
C	0	50
H	0	100
O	0	10
N	0	5

Formula Calculator Results

Formula	Best	Measured Mass	Tgt Mass	Diff (ppm)	Score
C21 H30 N3 O6	True	420.2128	420.2129	0.19	95.76

(3) ESI-HRMS for **2PCA-PEG$_5$**

Spectra

Fragmentor Voltage	Collision Energy	Ionization Mode
100	0	ESI

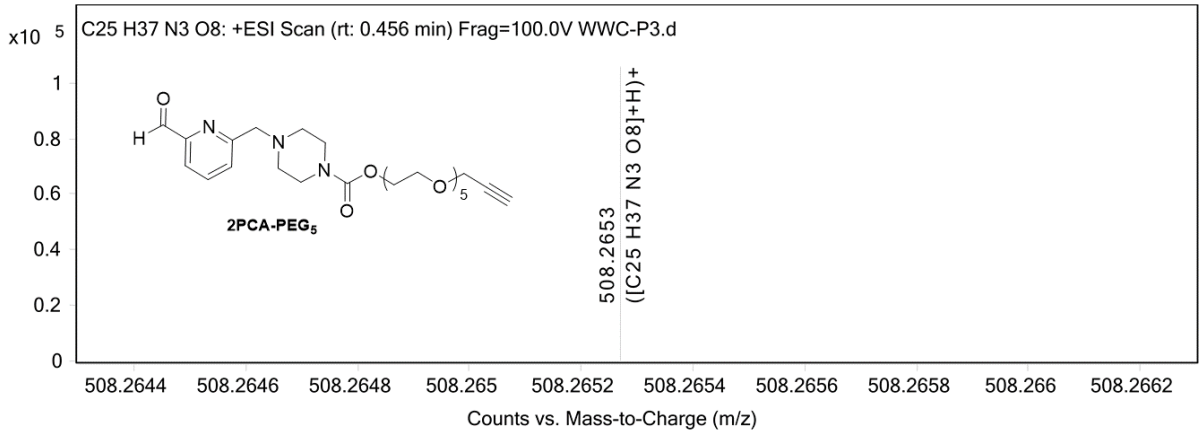

Formula Calculator Element Limits

Element	Min	Max
C	0	50
H	0	100
O	0	10
N	0	5

Formula Calculator Results

Formula	Best	Measured Mass	Tgt Mass	Diff (ppm)	Score
C25 H38 N3 O8	True	508.2653	508.2653	0.03	99.69

(4) ESI-HRMS for **SRB-N$_3$**

Spectra

Fragmentor Voltage	Collision Energy	Ionization Mode
100	0	ESI

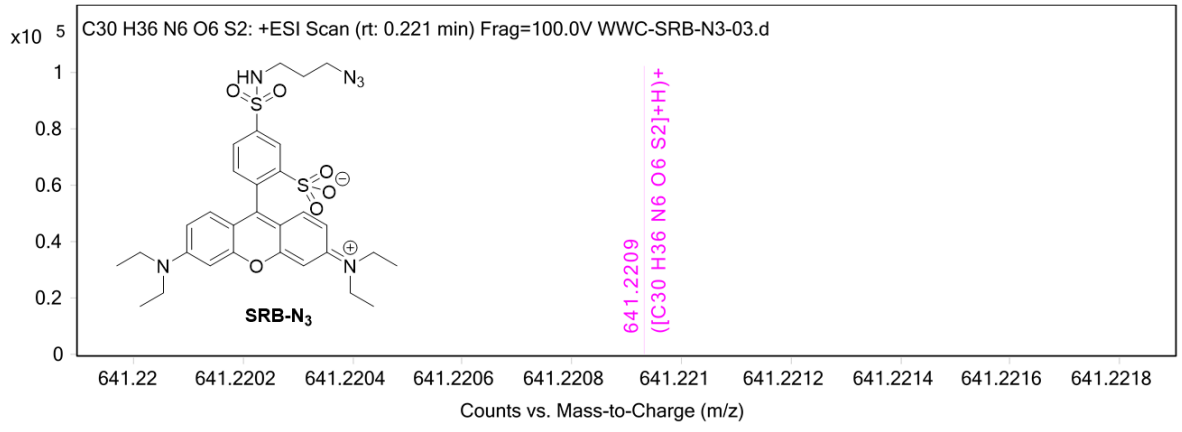

SRB-N_3

Formula Calculator Element Limits

Element	Min	Max
C	0	50
H	0	100
O	0	10
N	6	6
S	2	2

Formula Calculator Results

Formula	Best	Measured Mass	Tgt Mass	Diff (ppm)	Score
C30 H37 N6 O6 S2	True	641.2209	641.2211	-0.15	95.39